LETTER

Temporal variability of forest communities: empirical estimates of population change in 4000 tree species

Ryan A. Chisholm,[1,2]* Richard Condit,[1] K. Abd. Rahman,[3] Patrick J. Baker,[4] Sarayudh Bunyavejchewin,[5] Yu-Yun Chen,[6] George Chuyong,[7] H. S. Dattaraja,[8] Stuart Davies,[9] Corneille E. N. Ewango,[10] C. V. S. Gunatilleke,[11] I. A. U. Nimal Gunatilleke,[11] Stephen Hubbell,[1,12] David Kenfack,[9] Somboon Kiratiprayoon,[13] Yiching Lin,[14] Jean-Remy Makana,[10] Nantachai Pongpattananurak,[15] Sandeep Pulla,[8] Ruwan Punchi-Manage,[16] Raman Sukumar,[8] Sheng-Hsin Su,[17] I-Fang Sun,[6] H. S. Suresh,[8] Sylvester Tan,[9] Duncan Thomas[18] and Sandra Yap[19]

Abstract

Long-term surveys of entire communities of species are needed to measure fluctuations in natural populations and elucidate the mechanisms driving population dynamics and community assembly. We analysed changes in abundance of over 4000 tree species in 12 forests across the world over periods of 6–28 years. Abundance fluctuations in all forests are large and consistent with population dynamics models in which temporal environmental variance plays a central role. At some sites we identify clear environmental drivers, such as fire and drought, that could underlie these patterns, but at other sites there is a need for further research to identify drivers. In addition, cross-site comparisons showed that abundance fluctuations were smaller at species-rich sites, consistent with the idea that stable environmental conditions promote higher diversity. Much community ecology theory emphasises demographic variance and niche stabilisation; we encourage the development of theory in which temporal environmental variance plays a central role.

Keywords

Abundance fluctuations, biodiversity, demographic stochasticity, environmental variance, forest dynamics, neutral theory, niche stabilization.

Ecology Letters (2014)

INTRODUCTION

There was a time when the prevailing scientific view was that ecological communities were stable over time, but this is now long past (Connell 1978; Sprugel 1991; Wright 2005; Laurance *et al.* 2009). Climatic shifts alter species assemblages, certainly over glacial cycles (Colinvaux *et al.* 1996), but also with modern anthropogenic climate change (Condit *et al.* 1996). Outbreaks of pests and pathogens that cause major abundance shifts are no longer considered abnormal. There is, however, considerable disagreement over the relative importance of different mechanisms that cause species abundances to fluctuate, especially given the increased frequency and intensity of anthropogenic disturbances (Wright 2005).

Two broad classes of stochasticity that may cause species' abundances to fluctuate temporally are environmental and demographic variance (Bjørnstad & Grenfell 2001; Lande *et al.* 2003; Melbourne & Hastings 2008; Gravel *et al.* 2011). Temporal environmental variance (henceforth 'environmental variance') arises from external drivers such as fluctuations in rainfall, temperature, fire and pests. The effect of environmental variance is correlated across individuals within species because conspecifics exhibit similar responses to the environment. Thus, environmental variance may be important for large populations as well as small populations. Demographic variance can be subdivided into demographic stochasticity, which arises from the discreteness of individuals and the random nature of birth and death processes, and demographic

[1]*Smithsonian Tropical Research Institute, P.O. Box 0843-03092, Balboa, Ancón, Republic of Panamá*

[2]*Department of Biological Sciences, Faculty of Science, National University of Singapore, 14 Science Drive 4, Singapore, 117543, Singapore*

[3]*Forest Research Institute Malaysia, 52109, Kepong, Selangor Darul Ehsan, Malaysia*

[4]*Department of Forest and Ecosystem Science, University of Melbourne, 500 Yarra Boulevard, Richmond, 3121, Vic., Australia*

[5]*Research Office, Department of National Parks, Wildlife and Plant Conservation, Bangkok, 10900, Thailand*

[6]*Department of Natural Resources and Environmental Studies, National Dong Hwa University, Hualien, 97401, Taiwan.*

[7]*Department of Botany and Plant Physiology, University of Buea, PO Box 63, Buea, SWP, Cameroon*

[8]*Centre for Ecological Sciences, Indian Institute of Science, Bangalore, 560012, India*

[9]*Smithsonian Institution Global Earth Observatory, Center for Tropical Forest Science, Smithsonian Institution, P.O. Box 37012, Washington, DC, 20013, USA*

[10]*Wildlife Conservation Society, Kinshasa/Gombe, DR Congo*

[11]*Faculty of Science, Department of Botany, University of Peradeniya, Peradeniya, 20400, Sri Lanka*

[12]*Department of Ecology and Evolutionary Biology, University of California, Los Angeles, CA, 90095, USA*

[13]*Faculty of Science and Technology, Thammasat University (Rangsit), Klongluang, Patumtani, Thailand*

[14]*Department of Life Science, Tunghai University, Taichung, 40704, Taiwan*

[15]*Department of Forest Biology, Faculty of Forestry, Kasetsart University, Chatuchak, Bangkok, 10900, Thailand*

[16]*Department of Ecosystem Modeling, University of Göttingen, Büsgenweg 4, 37077, Göttingen, Germany*

[17]*Taiwan Forestry Research Institute, Taipei, 10066, Taiwan*

[18]*Department of Botany and Plant Pathology, Oregon State University, Corvallis, OR, 97331, USA*

[19]*Institute of Biology, University of the Philippines, Diliman, Quezon City, Philippines*

Correspondence: E-mail: ryan.chis@gmail.com

heterogeneity, which arises when birth and death rates of individuals within a population vary by age, size, genotype, biotic neighbourhood or abiotic neighbourhood. Because the effects of demographic variance are uncorrelated across individuals they average out in large populations and are strongest in small populations.

The fluctuations in abundance caused by environmental and demographic variance may be damped by niches, which exert 'stabilising mechanisms' on populations (Chesson 2000; Adler *et al.* 2007). In the extreme case of strong stabilising mechanisms, species' abundances may be constrained within narrow ranges; in the more general case, species' abundances may still fluctuate broadly but in a bounded way, ensuring coexistence (Chesson 1978; Schreiber *et al.* 2011). The theoretical basis for niche stabilisation is that the size of each species' niche is determined by abiotic or biotic factors, such as resource constraints or predators, and that if a species becomes too common its per-capita growth rate declines because of resource limitation or increased predation, whereas if it becomes too rare the opposite occurs. The net effect is negative density dependence, which, by definition, leads to stabilisation.

The relative strengths of environmental variance and demographic variance in ecological communities, and the extent to which they are damped by stabilising mechanisms, remain poorly understood. One scenario is that a combination of environmental variance and weak niche stabilisation leads to storage effects (Chesson 2000) or temporal niches, whereby a rare species can benefit from favourable environmental conditions by expanding to fill its niche, but a common species cannot do so because it is already close to its carrying capacity. On this view, a species' abundance would be stabilised over timescales longer than the periodicity of environmental variance but not necessarily over shorter timescales. Another scenario is one in which environmental and demographic heterogeneity are low and niche stabilisation is weak so that abundances drift with demographic stochasticity: this is neutral theory (Hubbell 2001). However, another scenario is that environmental variance, demographic variance and nonlinear dynamics all interact to produce complex patterns of long-term change in abundances and community composition (Bjørnstad & Grenfell 2001). This latter perspective is prominent in the population dynamics literature (Bjørnstad & Grenfell 2001), but in the community ecology literature, particularly with regards to forest trees and other plants, there has been a greater focus on demographic variance (neutral theory) and niche stabilisation.

In this study, we focus on temporal abundance fluctuations of tree species in tropical and subtropical forests. These tree communities can be spectacularly diverse, with up to 1000 species in a 50 ha plot. Static patterns of diversity, such as the species abundance distribution, have been well studied in these forests (Hubbell 2001; Volkov *et al.* 2003; Adler *et al.* 2007), but temporal patterns have received less attention (Leigh 2007). Long-term forest plots (Condit 1998) provide a window into these temporal patterns and an opportunity to study tree population dynamics at unprecedented scales. Comparing abundance fluctuations across sites with different species richness and environmental conditions can also help to isolate the relative importance of environmental and demographic variance. Our data set comprises long-term records of fluctuations in tree species' abundance from 12 sites around the world. Our goal is to characterise the observed variability in these communities and thereby make general inferences about the processes driving population dynamics at different sites over decadal timescales.

MATERIALS AND METHODS

Data

At 12 sites across three continents (Condit 1998), we conducted complete censuses of tree communities over periods spanning 6–28 years, and we documented abundance changes in over 4000 species. The longest census period (28 years) was at Barro Colorado Island (BCI) in Panama. Each of our 12 census plots covers at least 16 ha of forest in which all stems with diameter-at-breast-height (DBH) 1 cm or greater (25 000–350 000 trees per plot; over 2 million trees in total) are marked and identified to species level (Table 1). Total tree species richness varies from ≈70 at a seasonal dry forest in India to over 1000 at an aseasonal wet forest in Southeast Asia (Table 2). Individual species vary in abundance from one (every plot has several such singletons) to more than 60 000.

Abundance fluctuations across species within sites

For a given site, denote by N_{it} the abundance of species i in census t. We investigated the scaling of squared abundance changes $(N_{i,t+1} - N_{it})^2$ with initial abundance (N_{it}) and compared it to theoretical predictions. To make theoretical predictions, we used models of population change incorporating demographic variance and environmental variance.

Demographic variance

Theory predicts that if demographic variance is the primary mechanism driving population dynamics then variance in abundance change should scale linearly with abundance (Lande *et al.* 2003; Engen *et al.* 2005). Therefore, a simple way to test the hypothesis that demographic variance drives population dynamics is to look at the exponent of the scaling relationship between variance in abundance change and abundance. We performed this test in the context of a model of demographic variance that is mechanistic and thus also provides confidence intervals on abundance changes. The model is a neutral model, in which by definition the demographic parameters are the same across all species (Hubbell 2001; Volkov *et al.* 2003). We used binomial survival, which assumes that mortality events are independent across individuals, and Poisson recruitment, which assumes that recruitment events are independent across individuals and across time [these distributions are standard in models of demographic variance: Melbourne 2012; using binomial recruitment instead makes no qualitative difference to the results (not shown)]:

$$N_{i,t+1} \sim \text{Bi}(N_{it}, 1 - \beta) + \text{Pois}(N_{it}\beta) \tag{1}$$

Here β is both the per-capita mortality and per-capita recruitment rate. The tilde symbol in eqn 1 means 'is distributed as'. From the model described by eqn 1, we obtain $E(N_{i,t+1}) = E(N_{i,t})$ and hence

Table 1 Study sites ordered by latitude (further details at http://www.ctfs.si.edu/)

Site name	Location	Latitude	Longitude	Rainfall (mm/year)	Area (ha)	Census period
Ituri	Congo	1.43°N	28.58°E	1682	40	1995–2007
Pasoh	Malaysia	2.98°N	102.31°E	1788	50	1987–2005
Lambir	Malaysia	4.19°N	114.02°E	2664	52	1992–2008
Korup	Cameroon	5.07°N	8.85°E	5272	50	1998–2008
Sinharaja	Sri Lanka	6.40°N	80.40°E	5016	25	1995–2007
Khao Chong	Thailand	7.54°N	99.80°E	2696	24	2000–2010
BCI	Panama	9.15°N	79.85°W	2551	50	1982–2010
Mudumalai	India	11.60°N	76.53°E	1249	50	1988–2000
HKK	Thailand	15.63°N	99.22°E	1476	50	1993–2009
Palanan	Philippines	17.04°N	122.39°E	3380	16	1998–2010
Fushan	Taiwan	24.76°N	121.56°E	4271	25	2004–2009

BCI, Barro Colorado Island; HKK, Huai Kha Khaeng; Ituri site includes Edoro and Lenda plots.

$$E\left((N_{i,t+1} - N_{it})^2 | N_{it}\right) = \mathrm{var}\left(N_{i,t+1} - N_{it} | N_{it}\right) = N_{it}\beta(2 - \beta) \quad (2)$$

where $\mathrm{var}(X|Y)$ indicates the variance of X given Y and we have used the identity $\mathrm{var}(X - Y|Y) = \mathrm{var}(X|Y)$. Because of the neutrality assumption, eqn 2 can be interpreted as either variance across time or variance across species.

Our neutral model (eqn 1) ignores immigration, which is justified as a first approximation because previous work suggests that immigrants into these forest plots constitute only ≈10% of recruits (Chisholm & Lichstein 2009). It also assumes that the community size is not changing directionally over time (because per-capita mortality equals per-capita recruitment), which is a necessary assumption in a model of strictly demographic variance (directionally varying total community size would by contrast imply synchronous environmental variance; see Appendix S1).

For each census interval at each site, we estimated the parameter β in eqn 1 as the average of observed overall per-capita recruitment and mortality rates and compared the squared abundance fluctuations predicted by the neutral model (eqn 2) to observations.

Environmental variance

The simplest models of environmental variance predict that abundance changes should scale quadratically with initial abundance (Lande *et al.* 2003). This is for the idealised case of no density dependence and perfectly correlated responses to the environment across individuals within species. Mathematically, this can be written as

$$N_{i,t+1} \sim R_i N_{it} \quad (3)$$

Here R_i is a random variable representing temporal variation in the response of species i to the environment (we ignore the unrealistic special case of eqn 3 where the R_i are time-invariant and each species undergoes exponential growth or decay). The index i on R_i means that the distribution of responses to the environment differs across species. The quadratic scaling of the variance in abundance change with initial abundance can be derived directly from eqn 3:

$$\mathrm{var}(N_{i,t+1} - N_{it} | N_{it}) = N_{it}^2 \mathrm{var}(R_i)$$

And it follows that squared abundance changes also scale quadratically with initial abundance:

$$\begin{aligned}
E\left((N_{i,t+1} - N_{it})^2 | N_{it}\right) = & \ \mathrm{var}(N_{i,t+1} - N_{it} | N_{it}) + \\
& E(N_{i,t+1} - N_{it} | N_{it})^2 \\
= & \ N_{it}^2 \{\mathrm{var}(R_i) + (E(R_i) - 1)^2\}
\end{aligned} \quad (4)$$

This idealised case of environmental variance serves as a bound on the kind of dynamics we might expect natural populations to exhibit. In more general models that include demographic variance as well, one expects to see power-law scaling with exponents somewhere between 1.0 (the idealised demographic-variance case of eqn 2) and 2.0 (the idealised environmental-variance case of eqn 4). In more general models that include niche-based negative density dependence (all of our models here are density-independent) or immigration, the exponent again may be substantially less than 2.0 and even less than 1.0, because negative density dependence by definition reduces the population growth rates of common species and elevates those of rare species. We did not consider niche-based negative density dependence or immigration in our models (because measured exponents were close to 2.0, suggesting these processes play relatively minor roles; see Results and Discussion).

Our environmental variance model (eqn 3) describes abundance changes over time of a single species given a distribution of population growth rates R_i (i.e. responses to the environment). In our data for each site, we do not have multiple data points for a single species (although we have multiple censuses, these are not really independent time points because they occur within a single tree generation), but single data points for many species. In this case, the scaling of abundance changes with abundance may deviate from the quadratic scaling predicted by eqn 4 because the distribution of population growth rates may be different for each species. In particular, a species' abundance may not be independent of its distribution of responses to the environment, and responses to the environment may be correlated across species. With these limitations in mind, we compared eqn 4 to the multispecies data at each site in each census

Table 2 Fits of the full population model to tree population change data at each site for each census interval (see Tables S1 and S2 for extended information)

Site and census interval		Species richness	Fitted intrinsic population growth rate (ρ) (year^{-1}) with quantiles			Fitted mean mortality (μ) (year^{-1})	Variance estimates	
			Centre	2.5%	97.5%		Env. (v_e) (year^{-2} indiv^{-2})	Dem. (v_d) (year^{-1} indiv^{-1})
Edoro	1–2	354	−0.0075	−0.0370	0.0526	0.0277	0.000468	0.0556
Edoro	2–3	362	−0.0081	−0.0385	0.0729	0.0336	0.000745	0.0718
Edoro	1–3	354	−0.0058	−0.0418	0.0520	0.0301	0.000498	0.0598
Lenda	1–2	346	−0.0005	−0.0338	0.0172	0.0250	0.000150	0.0456
Lenda	2–3	353	−0.0059	−0.0537	0.0306	0.0331	0.000398	0.0575
Lenda	1–3	346	−0.0018	−0.0568	0.0195	0.0299	0.000348	0.0496
Pasoh	1–2	811	−0.0107	−0.0278	0.0054	0.0193	0.000062	0.0277
Pasoh	2–3	811	−0.0073	−0.0240	0.0470	0.0268	0.000309	0.0557
Pasoh	3–4	814	−0.0082	−0.0501	0.0042	0.0337	0.000182	0.0517
Pasoh	4–5	814	−0.0147	−0.0461	0.0538	0.0344	0.000588	0.0636
Pasoh	1–5	808	−0.0088	−0.0364	0.0197	0.0252	0.000176	0.0418
Lambir	1–2	1197	0.0054	−0.0132	0.0396	0.0165	0.000161	0.0423
Lambir	2–3	1203	−0.0001	−0.0228	0.0614	0.0263	0.000425	0.0621
Lambir	3–4	1203	−0.0030	−0.0103	0.0654	0.0231	0.000393	0.0588
Lambir	1–4	1197	0.0024	−0.0149	0.0445	0.0174	0.000210	0.0434
Korup	1–2	490	−0.0043	−0.0333	0.0350	0.0255	0.000263	0.0492
Sinharaja	1–2	222	−0.0060	−0.0546	0.0237	0.0241	0.000349	0.0375
Sinharaja	2–3	219	−0.0094	−0.0459	0.0058	0.0247	0.000157	0.0347
Sinharaja	1–3	222	−0.0083	−0.0531	0.0122	0.0247	0.000251	0.0351
Khaochong	1–2	584	−0.0036	−0.0377	0.0475	0.0312	0.000411	0.0630
Khaochong	2–3	574	−0.0087	−0.0348	0.0365	0.0332	0.000292	0.0624
Khaochong	1–3	584	−0.0037	−0.0463	0.0314	0.0333	0.000338	0.0609
BCI	1–2	305	0.0072	−0.1102	0.0689	0.0613	0.001848	0.1159
BCI	2–3	304	0.0010	−0.0738	0.0757	0.0545	0.001239	0.1099
BCI	3–4	304	−0.0060	−0.0915	0.0299	0.0571	0.000870	0.0958
BCI	4–5	303	−0.0185	−0.0749	0.0738	0.0581	0.001258	0.1066
BCI	5–6	301	−0.0143	−0.0442	0.0948	0.0532	0.001205	0.1121
BCI	6–7	299	−0.0086	−0.0319	0.1120	0.0497	0.001349	0.1154
BCI	1–7	305	−0.0042	−0.0697	0.0467	0.0507	0.000761	0.0936
Mudumalai	1–2	69	−0.0049	−0.2084	0.0134	0.0871	0.003432	0.1218
Mudumalai	2–3	64	−0.0046	−0.2362	0.0546	0.0916	0.005318	0.1351
Mudumalai	3–4	65	−0.0081	−0.0920	0.2439	0.0588	0.006831	0.1517
Mudumalai	1–4	68	−0.0090	−0.1560	0.0906	0.0634	0.003424	0.1059
HKK	1–2	294	−0.0074	−0.1184	0.0796	0.0671	0.002213	0.1208
HKK	2–3	285	−0.0095	−0.0495	0.2302	0.0359	0.005152	0.1130
HKK	3–4	283	−0.0004	−0.0402	0.2091	0.0670	0.004048	0.1767
HKK	1–4	293	−0.0016	−0.0644	0.1259	0.0465	0.002103	0.1077
Palanan	1–2	308	0.0125	−0.0029	0.1723	0.0204	0.002126	0.0902
Palanan	2–3	317	−0.0123	−0.0408	0.0398	0.0288	0.000374	0.0513
Palanan	1–3	308	0.0020	−0.0140	0.0827	0.0231	0.000606	0.0646
Fushan	1–2	110	−0.0019	−0.0705	0.0554	0.0423	0.000888	0.0799

The environmental and demographic variance components (v_e and v_d) are estimated as described in the main text and Appendix S3.

interval by fitting a power law of the form $y = ax^2$ to the data, where y is the squared abundance change $(N_{i,t+1} - N_{i,t})^2$ and x is the initial abundance $N_{i,t}$. This tests whether tree population dynamics on decadal timescales can be approximated by a simple model of environmental variance that ignores immigration, species differences and density dependence.

Abundance fluctuations within species across sites

We then conducted a similar analysis within species across sites, i.e. we looked at how abundance fluctuations scaled with abundance for species that were present at more than one site. We restricted this analysis to our Asian sites, which have substantial species overlap. Again, under the hypothesis that

demographic variance is the major driver of population dynamics the scaling should have exponent 1.0, whereas under the hypothesis that environmental variance is the major driver the scaling should have exponent 2.0. The small number of data points per species prevented us from analysing each species independently; instead we used a linear mixed effects model with species as a random effect to estimate an average scaling exponent for all species.

Cross-site comparisons of overall variability in abundance fluctuations

We then compared the overall patterns of abundance fluctuations across forests to see whether some forests were more

variable than others. In these analyses, we considered relative abundances ($x_{it} = N_{it}/\sum_j N_{jt}$) rather than absolute abundances because the total community size varies substantially across forests and so, for example, an abundance of 10 in one forest may not have the same biological significance as an abundance of 10 in another forest (note, though, that we did repeat the analyses with absolute abundances to check robustness). In making direct comparisons across sites, we had to control for large cross-site variation in total species richness and distributions of relative abundances. To achieve this, we binned species into $\log_{10}$ relative abundance classes and compared fluctuations only within relative abundance classes across sites. So, for example, we compared the abundance fluctuations of species comprising 1–10% of the community at BCI with the abundance fluctuations of species comprising 1–10% of the community at Pasoh, and so on.

Partitioning demographic and environmental variance

The analyses described above suggested that a mix of demographic and environmental variance was driving the observed fluctuations, and so we sought to estimate these two variance components for each forest using a statistical model, the details of which are presented in the Supporting information (Appendices S2–S5). Briefly, we created the statistical model by modifying the neutral population dynamics eqn 1 so that mortality and recruitment rates were distinct and could vary across species, and then we specified functional forms for the distributions of the annualised mortality and recruitment rates: we described mortality with a lognormal distribution (Condit *et al.* 2006) and the difference between recruitment and mortality (i.e. the population growth rate) with an asymmetric Laplace (exponential) distribution (Appendix S4). We then fitted the statistical model to the annualised rates using Bayesian hierarchical methods. The fitted variance terms were decomposed into environmental and demographic variance using standard techniques (Appendix S3).

There are several limitations to this fitted abundance fluctuation model, mostly arising from the short length of our time series (maximum 28 years) relative to a tree generation ($\approx$50–100 years): (1) The true survival and recruitment distributions would be more complicated than binomial and Poisson distributions. (2) Our fitted environmental variance distribution confounds variation in abundance fluctuations across species with variation within species. (3) The short length of the time series allowed us to fit environmental variance in recruitment or mortality but not both: we chose the former for reasons explained in Appendix S3. (4) Demographic heterogeneity could only be fitted in an approximate way (Appendix S3). (5) The model ignores immigration, possibly inflating estimates of environmental variance. Thus, the fitted model should be viewed as a statistical analysis providing a first approximation to the demographic and environmental variances in these forests within the limitations of the data, rather than a comprehensive model capturing all relevant biological detail. The output of the fitted model should be interpreted in conjunction with the analyses on the raw data described in the previous sections.

RESULTS

Scaling of abundance fluctuations across species within sites

At every site, the scaling of abundance fluctuations with abundance over a single census interval was intermediate between that predicted by a neutral model (pure demographic stochasticity; exponent 1.0) and a model of environmental variance (exponent 2.0) (Fig. 1, Figs. S2–S3). More specifically, common species' abundance fluctuations were roughly consistent with the scaling predicted by the environmental variance model, whereas rare species' abundance fluctuations were more consistent with the neutral model. This suggests that rare species' dynamics are dominated by demographic stochasticity, whereas common species' dynamics are dominated by environmental variance. We also found that abundance fluctuations appear to have a large asynchronous component (Appendix S1; Fig. S1; see also Table S1).

The same overall patterns held when we looked at the longest time interval available in sites where more than two censuses had been conducted (Fig. 2), i.e. common species' dynamics appeared to be driven predominantly by environmental variance whereas rare species' dynamics appeared to be driven predominantly by demographic variance.

Scaling of abundance fluctuations within species across sites

Patterns of abundance fluctuations within species across our Asian sites were consistent with those observed in the within-site analyses: demographic variance dominated at low abundance and environmental variance dominated at high abundance (466 species were present at two or more of our Asian sites). Specifically, the estimated exponent of the power law relationship from all the data was 1.160 ± 0.038 (mean $\pm$ standard error), indicating a predominance of demographic variance, but when only common species were considered, the exponent was close to 2.0, indicating a predominance of environmental variance (Fig. 3).

Cross-site comparisons of overall variability in abundance fluctuations

In cross-site comparisons, we observed that the rarest species, those comprising less than 1/10 000th of a community, fluctuated to a similar degree regardless of site species richness (Fig. 4). In contrast, the common species, those comprising more than 1/1000th of a community, were much more variable at species-poor sites than at species-rich sites (Fig. 4). Similar results were obtained when we used absolute rather than relative abundances (not shown). As a rough rule of thumb, our data suggest that abundance fluctuations of common species are roughly four times as big in a forest of 100 species as in a forest with 1000 species (based on fitted lines in Fig. 4).

Partitioning demographic and environmental variance

The fitted model provided a quantitative decomposition of the annualised demographic (v_d) and environmental variance (v_e)
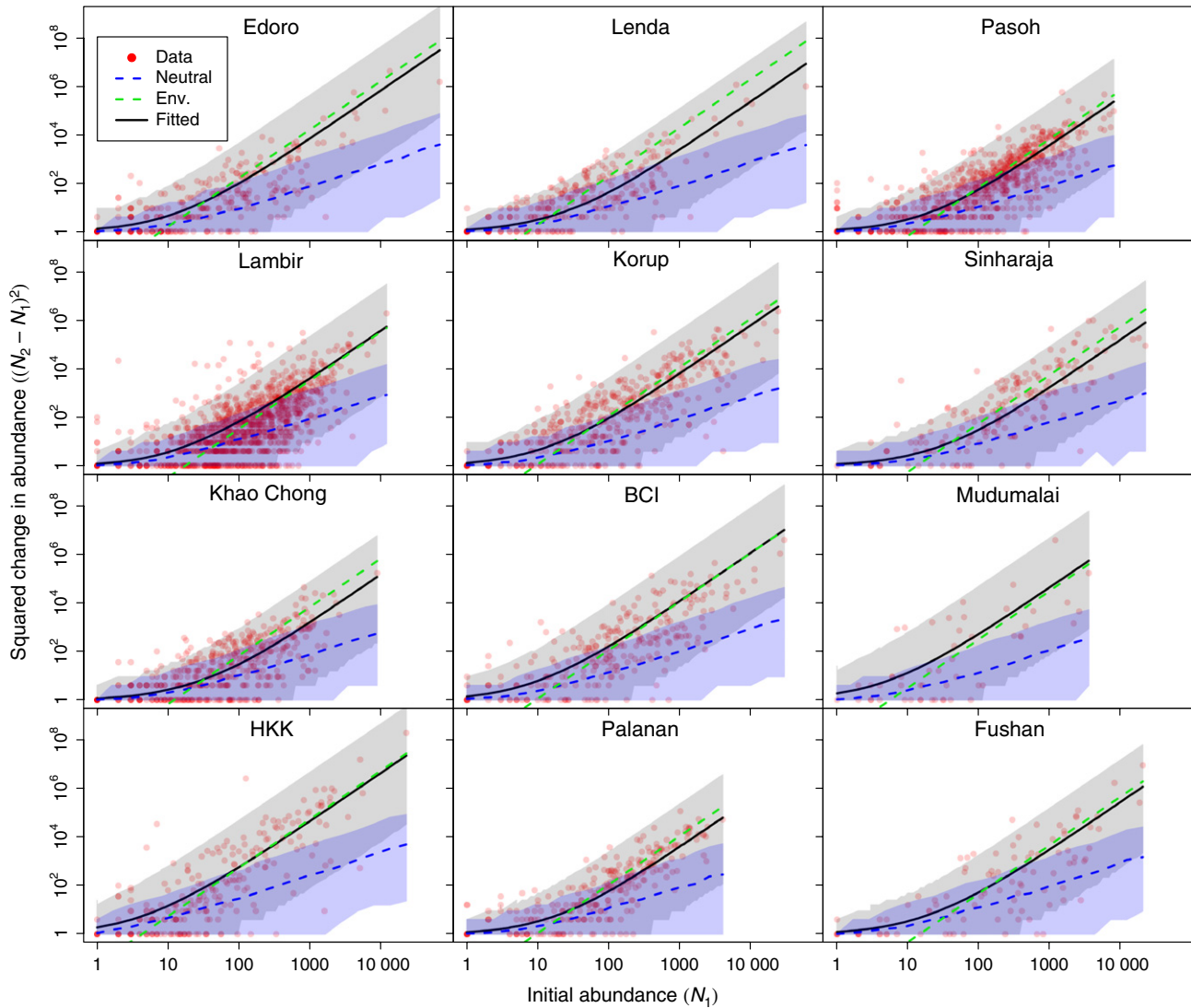
Figure 1 Squared abundance changes (vertical axes; log scale) as a function of initial abundance (horizontal axes; log scale) in 12 forests (panels) over a single census interval. Each panel corresponds to the most recent census at one site, with each red point showing data for one species. Blue dashed lines with shaded 95% confidence intervals show the predictions of neutral models. Green dashed lines show a best-fit power law with exponent 2.0, which corresponds to a model where the effects of environmental variance are perfectly correlated across individuals within species. Black curves with shaded 95% confidence intervals show the fitted model (see text). Species whose abundances did not change ($(N_2 - N_1)^2 = 0$) are not shown on the log axes. Note that abundances are directly comparable across sites only for sites that have the same area (see Table 1).

components and confirmed the results from the main analyses (Tables 2, S2). Specifically, there was a mix of environmental and demographic variance at all sites (consistent with the within-site analyses above), and variance tended to be higher in species-poor sites (consistent with the cross-site comparisons above). The fitted model adequately captured the variation in the data at most sites and census intervals, and clearly illustrated the transition from dynamics dominated by demographic variance at low abundances to dynamics dominated by environmental variance at high abundances (Figs. 1–2, S2–S3). Exceptions to the good model fit occurred in a few census intervals where the empirically observed abundances of rare species were unusually stable, causing the fitting procedure to underestimate environmental variance (Pasoh 1–2, Pasoh 3–4 and Mudumalai 1–2; Figs. S2–S3). Our estimates of

demographic variance v_d and environmental variance v_e (Table 2) can be used to estimate the range of possible abundance fluctuations given a species' initial abundance (see Appendix S6; these methods were used to construct the black curves with gray confidence intervals in Figs. 1–2).

DISCUSSION

The role of environmental variance as a driver of population dynamics has been highlighted in previous studies of birds, marine fish, plankton and other taxa (Bjørnstad & Grenfell 2001; Lande *et al.* 2003). In forest tree communities, environmental variance has also been identified as an important driver in some cases (e.g. Sukumar *et al.* 2005; Baker *et al.* 2008; Suresh *et al.* 2010), but theoretical work on forest dynamics
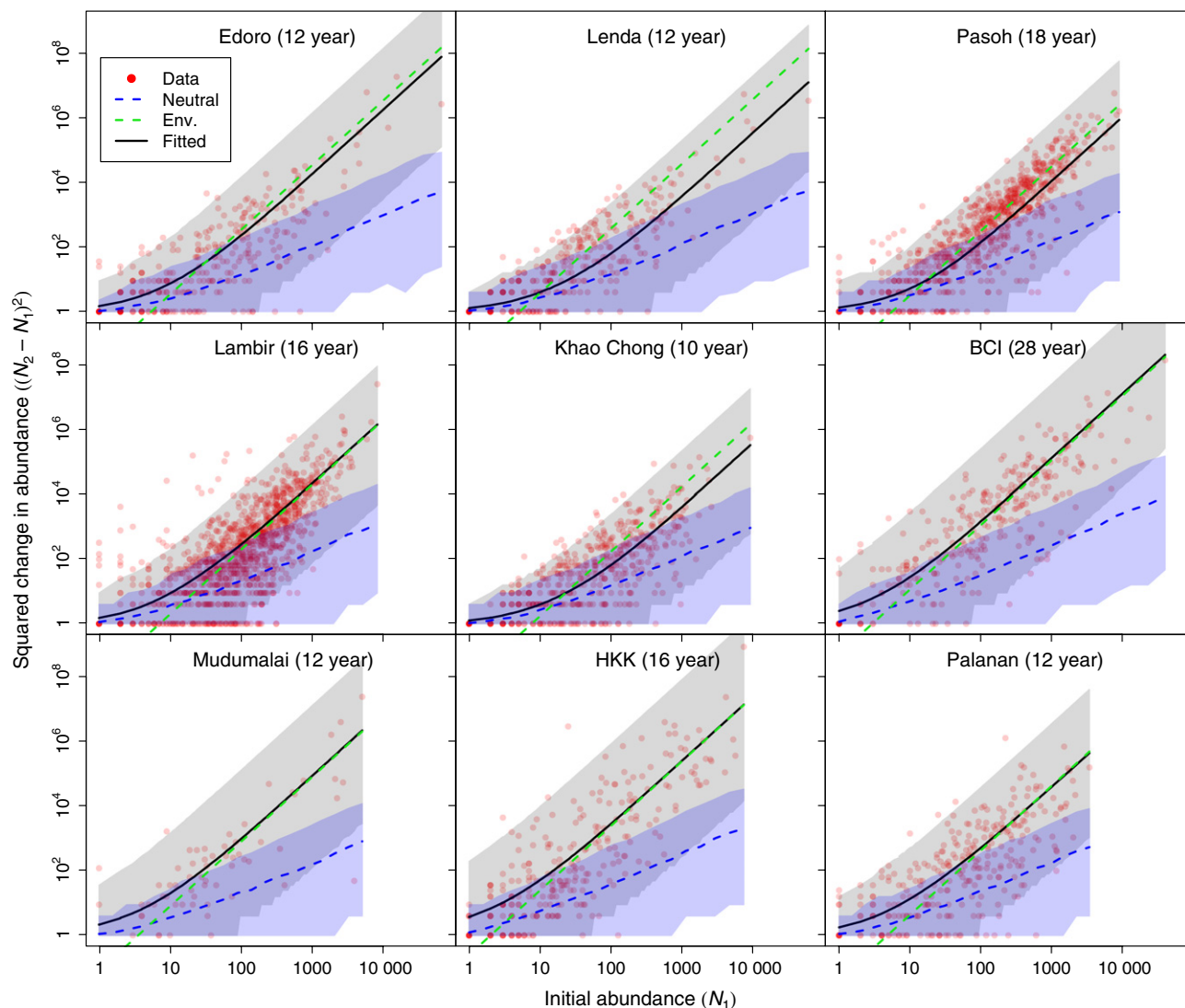
Figure 2 As for Fig. 1, but over the longest time interval available (rather than the most recent census) at sites where more than two censuses have been conducted. Panel titles show site name and length of interval.

and community assembly has remained centred on demographic variance (e.g. neutral theory) and niche stabilisation. Our long-term large-scale data set (over 2 million individuals of 4000 species in 12 forests on three continents) shows that environmental variance is consistently the largest factor driving tree population dynamics on decadal timescales. The line of reasoning that leads to this conclusion is that (1) Environmental variance induces temporal fluctuations in mortality and reproduction rates that are correlated across individuals within species, because individuals within species respond similarly to the environment (Lande *et al.* 2003); (2) Theory predicts that squared abundance changes should scale as the second power of abundance in the extreme case of perfectly correlated responses to the environment within species, density independence, no demographic variance and no systematic relationship between abundance and response to the environment (eqn 3) and (3) Squared abundance changes in our data set do indeed scale roughly as the second power of abundance

(Figs. 1–3), at least for large abundances where the effects of demographic variance are expected to be weak. Theoretical models of population dynamics centred on other processes, such as demographic variance, niche-based negative density dependence and nonlinear interspecific interactions (see below), predict different scalings. Thus, while these other processes do operate in forest tree communities (e.g. Hubbell 2001; Wright 2002; Comita *et al.* 2010; Mangan *et al.* 2010) and are necessary for a holistic understanding of population dynamics, their effects appear to be weak relative to those of environmental variance on decadal timescales. In addition, we found that abundance fluctuations across species have a large asynchronous component, i.e. relative and not just absolute abundances are fluctuating, which means that environmental variance plays a key role in determining community composition.

Processes that lead to environmental variance include drought, fires and storms, but also insect and fungus out-
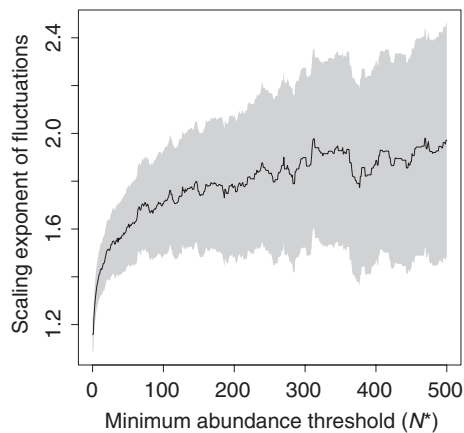
Figure 3 Scaling of abundance changes within species for 466 species that occurred at two or more of our Asian sites. The vertical axis indicates the estimated exponent of the relationship between squared abundance fluctuations (($N_2 - N_1)^2$) and initial abundance (N_1) within species using different minimum abundance thresholds (N^*; horizontal axis). The shaded region shows 95% confidence intervals on the exponent estimates. For low minimum abundance thresholds the exponent is close to 1.0, indicating a predominance of demographic variance. For high minimum abundance thresholds the exponent is close to 2.0, indicating a predominance of environmental variance.
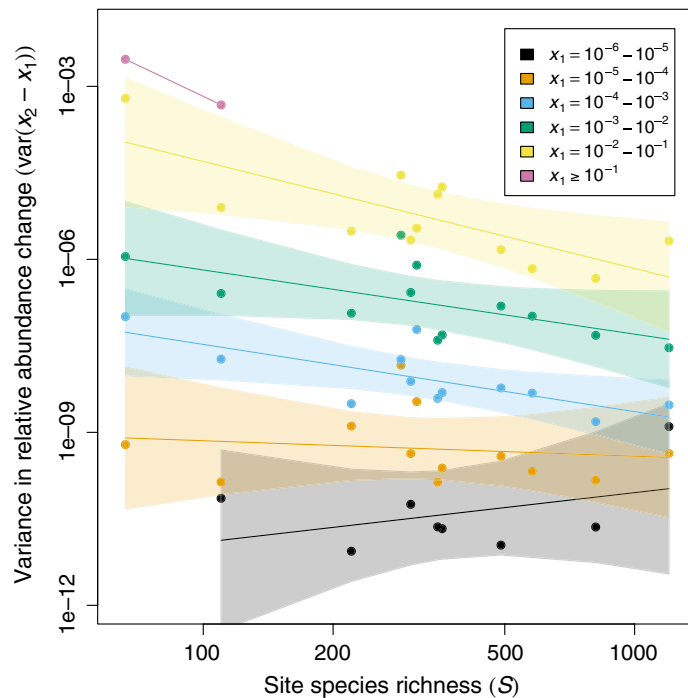
Figure 4 Cross-site comparison of forest variability versus species richness. Forest variability is measured as the variance of relative abundance changes (vertical axis) within $\log_{10}$ abundance classes (colours; see legend where x_1 = initial relative abundance). Each point corresponds to a single abundance class at a single site. Each coloured line with 95% confidence intervals shows the least-square fit to the corresponding relative abundance class (*P*-values associated with tests that the slope of each fitted line is statistically significantly different from zero are 0.318, 0.641, 0.007, 0.032, 0.004, from the lowest to the highest abundance class respectively).

breaks that may arise indirectly from environmental fluctuations. Among our 12 sites, environmental fluctuations driving tree population changes were in some cases conspicuous and have well-established causes. Typhoon Imbudo passed over the Palanan plot in 2003, and the census following showed high recruitment of several light-demanding species. In that census interval, the distribution of population fluctuations was skewed heavily toward the positive, with some species exhibiting population growth rates of $r = 14\%$ per year. However, while some species recruited well, many others did not, and some even declined in abundance: A typhoon does not lead to a uniform response across species, but a highly variable response. At Huai Kha Khaeng in Thailand, ground fires driven by the El Niño–Southern Oscillation (ENSO) burned through much of the plot in 1997–1998 near the end of the first census interval, promoting a recruitment pulse of fast-growing species and near complete loss of some fire-sensitive species (Baker *et al.* 2008). Other conspicuous fluctuations in populations were unexpected, but clearly attributable to external drivers. At BCI, a drought during the 1983 ENSO event caused high mortality in a few species, and the former canopy dominant *Poulsenia armata* suffered a 50% population loss over the following decade (Condit *et al.* 1996; Feeley *et al.* 2011). In the Mudumalai plot, four large fires (> 80% plot area burnt) during the first two census intervals resulted in high mortality primarily in the small-sized individuals, whereas elephant herbivory resulted in large population declines of favoured browse plants of the order Malvales (Sukumar *et al.* 2005; Suresh *et al.* 2010).

Several of the sites, in contrast, have witnessed no conspicuous fluctuations in climate or herbivory, particularly Pasoh and the three African sites. Nevertheless, tree species at these sites still exhibited large fluctuations in population size with a statistical signature of environmental variance (i.e. scaling of squared abundance changes as the second power of abundance; Fig. 1). Although these forests were more stable than the fire- and typhoon-impacted forests (Table 2, Fig. 1), there must still be environmental drivers that favoured some species over others during the time intervals considered. Weather variation is a likely candidate. Identifying specific weather-related mechanisms and other weaker drivers may, however, be difficult in tree communities because of the long generation times and the lack of data on past environmental conditions. The median age of 1 cm DBH stems on BCI has been estimated at 16.6 years with a maximum of about 80 years (Hubbell 1998), so the new recruits in any given forest census (stems that have reached 1 cm DBH in the last ≈5 years) reflect not just the environmental conditions of the current year or decade but instead a weighted integral over decades of variable environmental conditions. Acquiring data on environmental conditions over such timescales and developing statistical techniques to integrate over them in conjunction with the tree abundance data is challenging. It is worth noting that in annual plant communities, where much biodiversity theory has been developed, the shorter generation times reduce the time lags in species-environment interactions (Chesson & Huntly 1989) and make such analyses more tractable.

Our analysis also provides a potential answer to the long-standing ecological question of why some forests around the

world have much higher diversity than others (e.g. in our data set there is an almost 20-fold variation in species richness across forests). The data suggest that high tree diversity may be the result of a stable environment: mechanistically, stable environmental conditions lead to smaller fluctuations in abundance, which reduces the probability of extinction of rare species, and elevates diversity (Fig. 4). This is qualitatively similar to the hypothesis that the latitudinal biodiversity gradient (Hillebrand 2004) is explained by stable environmental conditions in the tropics and unstable environmental conditions in the temperate zone over geological time (Pianka 1966; McGlone 1996). We speculate, based on our results, that tropical diversity may be explained not just by environmental stability at one timescale (geological) but at several (e.g. decadal and geological).

The persistence of a strong signature of environmental variance on timescales of up to 28 years in these forests demonstrates a role for environmental processes that have periodicity longer than this or are non-stationary (Baker *et al.* 2005). A component of long-term cyclic variation arises from climate, which exhibits fluctuations such as those associated with ENSO (Condit *et al.* 1996; Cook *et al.* 2010). Long-term environmental variation may also arise from directional anthropogenic impacts such as climate change (Holmgren *et al.* 2001; Condit *et al.* 2004), altered nutrient deposition rates (Vitousek *et al.* 1997) or the extirpation of seed-dispersing frugivorous mammals (Wright *et al.* 2000).

We have stated that environmental variance is the most plausible mechanism for explaining the large abundance fluctuations observed in the tree data; we now briefly explain why alternative hypotheses are less plausible. The hypothesis that some unmodelled form of demographic heterogeneity could account for the observed large abundance fluctuations can be rejected because, as already noted, the effects of demographic variance should decay rapidly with population size (Lande *et al.* 2003), whereas we observe large fluctuations in abundant species at all sites (i.e. the power-law scaling with exponent ≈2.0; Fig. 1–2). We can also rule out the possibility that common species are systematically those with high demographic rates (Fig. 3). Another alternative hypothesis is that large abundance fluctuations are a signature of chaotic dynamics induced by nonlinear species interactions (Huisman & Weissing 2001). Under this hypothesis, the fluctuations are driven not by external environmental factors but by the intrinsic process of competition between tree species, e.g. the heavy mortality of the former BCI canopy dominant *Poulsenia armata* in the 1980s would be attributed not to the 1983 drought but to the rise of another tree species that has a negative effect on *Poulsenia* or the decline of a species that has a positive effect on it, and the rise and decline of these species would be attributed to earlier rises and declines of other species. Such dynamics may well play some role in our forests, but we expect that they are less important than environmental drivers because most pairwise species interactions are inevitably weak in high-diversity communities of sedentary individuals (e.g. trees). Techniques for distinguishing chaos from stochasticity could resolve this issue more definitively (Sugihara & May 1990) but would require longer time series (e.g. from pollen cores).

What can the patterns of abundance fluctuations observed across tree species and across forests tell us about the major theories of forest tree diversity? We turn first to neutral theory (Hubbell 2001), which includes the processes of demographic stochasticity, speciation and dispersal, but ignores any niche differences or environmental effects. The tendency of neutral theory to perform well against static biodiversity patterns, but poorly against dynamic patterns has been noted previously in Panama (Condit *et al.* 1996; Leigh 2007) and the Amazon (Laurance *et al.* 2009). We can now say with more certainty that the failure of neutral theory's dynamical predictions in forests is general and not confined to particular species, sites or time periods (Fig. 1). Although neutral theory may adequately describe species abundance distributions (Volkov *et al.* 2003), species area curves (O'Dwyer & Green 2010) and immigration rates (Chisholm & Lichstein 2009; Condit *et al.* 2012), it clearly has a timescale problem (Nee 2005). It is not yet clear whether neutral theory's good static predictions are robust to the addition of environmental variance. Our results will facilitate the development of stochastic biodiversity models that can address these issues.

The second theory that our results can inform is niche stabilisation theory (Chesson 2000; Adler *et al.* 2007). Niche stabilisation theory holds that species' abundances are stabilised over time by negative density dependence arising from disease, predation or resource limitation (Comita *et al.* 2010; Mangan *et al.* 2010; Chisholm & Muller-Landau 2011). Stabilisation does not necessarily mean that species' abundances are stabilised within narrow ranges, because the dynamics can play out over long timescales: species can have good years and bad years, or good decades and bad decades. Indeed, these very fluctuations may allow a large number of species to persist in the system (i.e. storage effects or temporal niches; Chesson 2000). On this view, the large fluctuations observed in our forests would have been even larger had it not been for the effects of stabilising mechanisms. Our quantification of the variance terms (Table 2), may be useful for parameterising models of temporal niches to place bounds on the strengths and characteristic timescales of stabilisation forces in these tree communities.

In view of our results, we encourage the development of biodiversity and community assembly theory in which environmental variance has a more central role (Azaele *et al.* 2006; Ostling 2012). Niche stabilisation theories that allow species abundances to fluctuate broadly should be favoured over those that constrain species abundances within narrow ranges. Stochastic theories of community ecology, which have typically been based on demographic stochasticity and weak or absent niches (Hubbell 2001; Rosindell *et al.* 2011), should be extended to consider the combined effects of demographic and environmental variance. These proposals would also bring community ecology more in line with the literature on population dynamics, where there has been a greater emphasis on long-term change arising from the interaction of environmental variance, demographic variance and nonlinear dynamics (Bjørnstad & Grenfell 2001) and less emphasis on stability and neutrality.

AUTHORSHIP

R. A. C. and R. C. designed the study, performed analyses and wrote the manuscript. All other authors (listed alphabetically) collected the data, analysed the data and/or contributed to the scientific discussion.

REFERENCES

Adler, P.B., Hille Ris Lambers, J. & Levine, J.M. (2007). A niche for neutrality. *Ecol. Lett.*, 10, 95–104.

Azaele, S., Pigolotti, S., Banavar, J.R. & Maritan, A. (2006). Dynamical evolution of ecosystems. *Nature*, 444, 926–928.

Baker, P.J., Bunyavejchewin, S., Oliver, C.D. & Ashton, P.S. (2005). Disturbance history and historical stand dynamics of a seasonal tropical forest in western Thailand. *Ecol. Monogr.*, 75, 317–343.

Baker, P.J., Bunyavejchewin, S. & Robinson, A.P. (2008). The impacts of large-scale, low-intensity fires on the forests of continental Southeast Asia. *Int. J Wildland Fire*, 17, 782–792.

Bjørnstad, O.N. & Grenfell, B.T. (2001). Noisy clockwork: time series analysis of population fluctuations in animals. *Science*, 293, 638–643.

Chesson, P. (1978). Predator-prey theory and variability. *Annu. Rev. Ecol. Syst.*, 9, 323–347.

Chesson, P. (2000). Mechanisms of maintenance of species diversity. *Annu. Rev. Ecol. Syst.*, 31, 343–366.

Chesson, P. & Huntly, N. (1989). Short-term instabilities and long-term community dynamics. *Trends Ecol. Evol.*, 4, 293–298.

Chisholm, R.A. & Lichstein, J.W. (2009). Linking dispersal, immigration and scale in the neutral theory of biodiversity. *Ecol. Lett.*, 12, 1385–1393.

Chisholm, R. & Muller-Landau, H. (2011). A theoretical model linking interspecific variation in density dependence to species abundances. *Theor. Ecol.*, 4, 241–253.

Colinvaux, P.A., De Oliveira, P.E., Moreno, J.E., Miller, M.C. & Bush, M.B. (1996). A long pollen record from lowland Amazonia: forest and cooling in glacial times. *Science*, 274, 85–88.

Comita, L.S., Muller-Landau, H.C., Aguilar, S. & Hubbell, S.P. (2010). Asymmetric density dependence shapes species abundances in a tropical tree community. *Science*, 329, 330–332.

Condit, R. (1998). *Tropical Forest Census Plots: Methods and Results from Barro Colorado Island, Panama and a Comparison with Other Plots*. Springer-Verlag and R. G. Landes Company, Berlin, Germany, and Georgetown, Texas.

Condit, R., Hubbell, S.P. & Foster, R.B. (1996). Changes in tree species abundance in a Neotropical forest: impact of climate change. *J. Trop. Ecol.*, 12, 231–256.

Condit, R., Aguilar, S., Hernandez, A., Perez, R., Lao, S., Angehr, G. et al. (2004). Tropical forest dynamics across a rainfall gradient and the impact of an El Niño dry season. *J. Trop. Ecol.*, 20, 51–72.

Condit, R., Ashton, P., Bunyavejchewin, S., Dattaraja, H.S., Davies, S., Esufali, S. *et al.* (2006). The importance of demographic niches to tree diversity. *Science*, 313, 98–101.

Condit, R., Chisholm, R.A. & Hubbell, S.P. (2012). Thirty years of forest census at barro colorado and the importance of immigration in maintaining diversity. *PLoS ONE*, 7, e49826.

Connell, J.H. (1978). Diversity in tropical rain forests and coral reefs. *Science*, 199: 1302–1310.

Cook, E.R., Anchukaitis, K.J., Buckley, B.M., D'Arrigo, R.D., Jacoby, G.C. & Wright, W.E. (2010). Asian monsoon failure and megadrought during the last millennium. *Science*, 328, 486–489.

Engen, S., Lande, R., Saether, B.E. & Weimerskirch, H. (2005). Extinction in relation to demographic and environmental stochasticity in age-structured models. *Math. Biosci.*, 195, 210–227.

Feeley, K.J., Davies, S.J., Perez, R., Hubbell, S.P. & Foster, R.B. (2011). Directional changes in the species composition of a tropical forest. *Ecology*, 92, 871–882.

Gravel, D., Guichard, F. & Hochberg, M.E. (2011). Species coexistence in a variable world. *Ecol. Lett.*, 14, 828–839.

Hillebrand, H. (2004). On the generality of the latitudinal diversity gradient. *Am. Nat.*, 163, 192–211.

Holmgren, M., Scheffer, M., Ezcurra, E., Gutiérrez, J.R. & Mohren, G.M.J. (2001). El Niño effects on the dynamics of terrestrial ecosystems. *Trends Ecol. Evol.*, 16, 89–94.

Hubbell, S.P. (1998). The maintenance of diversity in a neotropical tree community: conceptual issues, current evidence, and challenges ahead. In: *Forest biodiversity research, monitoring and modeling: Conceptual background and old world case studies.* (eds Dallmeier, F., Comiskey, J.A.). Parthenon Publishing Pearl River, NY, pp. 17–44.

Hubbell, S.P. (2001). *The Unified Neutral Theory of Biodiversity and Biogeography*. Princeton University Press, Princeton, NJ.

Huisman, J. & Weissing, F.J. (2001). Fundamental unpredictability in multispecies competition. *Am. Nat.*, 157, 488–494.

Lande, R., Engen, S. & Saether, B.E. (2003). *Stochastic Population Dynamics in Ecology and Conservation*. Oxford University Press, Oxford, UK.

Laurance, S.G.W., Laurance, W.F., Henrique, E.M.N., Andrade, A., Fearnside, P.M., Expedito, R.G.R. et al. (2009). Long-term variation in Amazon forest dynamics. *J. Veg. Sci.*, 20, 323–333.

Leigh, E.G. (2007). Neutral theory: a historical perspective. *J. Evol. Biol.*, 20, 2075–2091.

Mangan, S.A., Schnitzer, S.A., Herre, E.A., Mack, K.M.L., Valencia, M.C., Sanchez, E.I. et al. (2010). Negative plant-soil feedback predicts tree-species relative abundance in a tropical forest. *Nature*, 466, 752–755.

McGlone, M.S. (1996). When history matters: Scale, time, climate and tree diversity. *Global Ecol. Biogeogr. Lett.*, 5, 309–314.

Melbourne, B.A. (2012). Stochasticity, demographic. In: *Encyclopedia of Theoretical Ecology* (eds Hastings, A. & Gross, L.J.), University of California Press, Berkeley, pp. 706–712.

Melbourne, B.A. & Hastings, A. (2008). Extinction risk depends strongly on factors contributing to stochasticity. *Nature*, 454, 100–103.

Nee, S. (2005). The neutral theory of biodiversity: do the numbers add up? *Funct. Ecol.*, 19, 173–176.

O'Dwyer, J.P. & Green, J.L. (2010). Field theory for biogeography: a spatially explicit model for predicting patterns of biodiversity. *Ecol. Lett.*, 13, 87–95.

Ostling, A.M. (2012). Large-scale spatial synchrony and the stability of forest biodiversity revisited. *J. Plant Ecol.*, 5, 52–63.

Pianka, E.R. (1966). Latitudinal gradients in species diversity - a review of concepts. *Am. Nat.*, 100, 33–46.

Rosindell, J., Hubbell, S.P. & Etienne, R.S. (2011). The unified neutral theory of biodiversity and biogeography at age ten. *Trends Ecol. Evol.*, 26, 340–348.

Schreiber, S.J., Benaim, J.M. & Atchade, K.A.S. (2011). Persistence in fluctuating environments. *J. Math. Biol.*, 63, 655–683.

Sprugel, D.G. (1991). Disturbance, equilibrium, and environmental variability: what is 'natural' vegetation in a changing environment? *Biol. Conserv.*, 58, 1–18.

Sugihara, G. & May, R.M. (1990). Nonlinear forecasting as a way of distinguishing chaos from measurement error in time-series. *Nature*, 344, 734–741.

Sukumar, R., Suresh, H.S., Dattaraja, H.S., Srinidhi, S. & Nath, C. (2005). The dynamics of a tropical dry forest in India: climate, fire, elephants and the evolution of life-history strategies. In: *Biotic interactions in the tropics: Their role in the maintenance of species diversity*. (eds Burslem, D.F.R.P., Pinard, M.A., Hartley, S.E.). Cambridge University Press, Cambridge, United Kingdom, pp. 510–529.

Suresh, H.S., Dattaraja, H.S. & Sukumar, R. (2010). Relationship between annual rainfall and tree mortality in a tropical dry forest: Results of a 19-year study at Mudumalai, southern India. *For. Ecol. Manage.*, 259, 762–769.

Vitousek, P.M., Mooney, H.A., Lubchenco, J. & Melillo, J.M. (1997). Human domination of Earth's ecosystems. *Science*, 277, 494–499.

Volkov, I., Banavar, J.R., Hubbell, S.P. & Maritan, A. (2003). Neutral theory and relative species abundance in ecology. *Nature*, 424, 1035–1037.

Wright, S.J. (2002). Plant diversity in tropical forests: a review of mechanisms of species coexistence. *Oecologia*, 130, 1–14.

Wright, S.J. (2005). Tropical forests in a changing environment. *Trends Ecol. Evol.*, 20, 553–560.

Wright, S.J., Zeballos, H., Dominguez, I., Gallardo, M.M., Moreno, M.C. & Ibanez, R. (2000). Poachers alter mammal abundance, seed dispersal, and seed predation in a neotropical forest. *Conserv. Biol.*, 14, 227–239.

SUPPORTING INFORMATION

Additional Supporting Information may be downloaded via the online version of this article at Wiley Online Library (www.ecologyletters.com).

Supporting Information: Temporal variability of forest communities: empirical estimates of population change in 4000 tree species

Appendix S1: Models of synchronous environmental variance

We tested whether the abundance fluctuations observed in our data could be explained by synchronous responses to environmental variance. Our tests were based on our model of demographic variance from the main text:

$$N_{i,t+1} \sim Bi(N_{it}, \zeta) + Pois(N_{it}\beta)$$

with $\zeta = 1 - \beta$. If we relax this latter assumption and use subscripts t to indicate that the recruitment probability β_t and survival probability ζ_t vary over time, this becomes a model of demographic variance and synchronous environmental variance. The reason this model exhibits synchronous environmental variance is that vital rates vary over time but are the same for all species at any given time. This leads to directional changes in the size of the community (as opposed to the random fluctuations around average community size observed when $\zeta = 1 - \beta$). Changes in species' relative abundance are largely synchronized in this model: any variation across species is due solely to demographic variance.

For each site and census interval we set the parameters β_t and ζ_t to the observed average per-capita recruitment and survival rates. We then generated random realizations of abundance changes from the model and compared these to the empirical data. We performed two statistical tests, the first focusing on the signs of abundance changes and the second focusing on the magnitudes (variances) of abundance changes. The result of the first test was that fewer species' abundances are moving in the same direction than one would expect based on the synchronous model: an average of 71.9% of species' abundances moved in the direction of the majority, and this was statistically significantly fewer than expected from the synchronous model in 26 out of 41 site-census-interval combinations at an $\alpha = 0.05$ significance threshold; 22 of these remained statistically significant at an $\alpha = 0.001$ significance threshold. The result of the second test was that the synchronous model severely underestimated the variation in abundance fluctuations across species in most cases (Fig. S1), even though it accurately captured the mean size of individual species' abundance fluctuations at several sites.

These results together indicate that the synchronous model is implausible at most sites and that there is therefore a strong component of asynchrony in tree species' responses to the environment. This led us to develop the model of environmental variance (described in the main text and Appendices S2–S5) that allows both synchronous and asynchronous changes. We later confirmed the inadequacy of models of synchronous environmental variance by comparing the AIC of the full fitted model versus the AIC of fitted synchronous models and finding that the former was always substantially lower (Table S1).

Appendix S2: Summary data

For a given forest site, denote by N_{it} the number of individuals of species i in census t, and by T_{it} the average date (measured in yr) on which individuals of species i were counted during census t (T_{it} is an average because individuals are typically censused over a range of dates). Then let $\Delta T_{it} = T_{i,t+1} - T_{it}$ be the census interval, measured in years, between successive counts. Finally let Z_{it} be the number of individuals of species i in census t that survived to census $t+1$. For each pair of censuses at each plot, the completed data table thus has a species name and four pieces of information: N_{it}, $N_{i,t+1}$, ΔT_{it} and Z_{it}. All species are included, encompassing all individual trees confidently assigned to a consistent taxonomic category. Many of the species are unnamed but recognizable as morphospecies. Rare species with $N_{it} = 0$ and $N_{i,t+1} > 0$ are excluded, because our final model ignores immigration (see below). There were few species in this category. For species with $N_{it} > 0$ and $N_{i,t+1} = 0$ we set $N_{i,t+1} = 0.01$ arbitrarily to allow these species to be included in the mathematical analysis.

For every species i, and for each census interval t, we calculated the rate of population change, r_{it}, which is the annual proportional change in population size from census t to $t+1$:

$$r_{it} = \frac{1}{\Delta T_{it}} \log\left(\frac{N_{i,t+1}}{N_{it}}\right)$$

(S)

We also estimated the annual mortality rate for each species i in each census interval t:

$$m_{it} = \frac{-1}{\Delta T_{it}} \log\left(\frac{Z_{it}}{N_{it}}\right)$$

(S)

Appendix S3: General model of abundance fluctuations

In the main text, our simplest model of population dynamics was a neutral model in which the per-capita survival rate $\zeta = 1 - \beta$ and reproductive rate β were the same for every species i:

$$N_{i,t+1} \sim Bi(N_{it}, \zeta) + Pois(N_{it}\beta)$$

In Appendix S1, we investigated the case where ζ and β vary across time, but are still constant across species: this was a model of synchronous environmental variance. Both the neutral model and the synchronous environmental variance model severely underpredicted the magnitude of abundance fluctuations in the data (Figs. 1–2, Figs. S1–S3).

More generally, we could imagine that the rates ζ and β would vary across individuals, species and time, and that there would be a density-independent immigration rate I_{it} that could vary across species and time:

$$N_{i,t+1} \sim I_{it} + \sum_{n=1}^{N_{it}} \left[Bi\left(1, \zeta_{i,t,n}\right) + Pois\left(\beta_{i,t,n}\right) \right]$$

(S)

where n sums over individuals. Because this model allows variation in vital rates across species and across individuals, it can potentially include demographic heterogeneity and environmental variance, in addition to demographic stochasticity. Eq. S can also be written as

$$N_{i,t+1} \sim I_{it} + PoisBi\left(\left\{\zeta_{i,t,n}\right\}\right) + Pois\left(\sum_{n=1}^{N_{it}} \beta_{i,t,n}\right)$$

where $PoisBi$ is the Poisson binomial distribution. The mean of the Poisson binomial distribution is the same as that of the corresponding binomial distribution with N_{it} trials and success probability $\acute{\zeta}_{it} = \frac{1}{N_{it}} \sum_n \zeta_{i,t,n}$. The variance of the Poisson binomial is less than that of the corresponding binomial, but the difference will be slight if the $\zeta_{i,t,n}$ are not too variable. For this reason, and because we lack sufficient independent time intervals to fit individual-level $\zeta_{i,t,n}$ and $\beta_{i,t,n}$ parameters to our data set, we instead work with mean $\acute{\zeta}_{it}$ and $\acute{\beta}_{it}$ parameters and approximate the above formula with

$$N_{i,t+1} \sim I_{it} + Bi\left(N_{it}, \acute{\zeta}_{it}\right) + Pois\left(N_{it} \acute{\beta}_{it}\right)$$

(S)

where $\acute{\beta}_{it} = \frac{1}{N_{it}} \sum_n \beta_{i,t,n}$. We reiterate that the only approximation made here is to replace the full Poisson binomial with a binomial that has an effective per-capita survival probability $\acute{\zeta}_{it}$. In our final model (see further down), this effectively means that demographic heterogeneity and demographic stochasticity are mixed together and cannot be estimated separately. This is necessary because the way to estimate demographic heterogeneity and demographic stochasticity separately would be to compare the variance and mean of the density-dependent component of survival over time and see how far they deviate from the binomial ideal, whereas in the present data we have only two independent time points so comparing the variance and mean in this way is not possible.

For the purposes of analyzing and fitting the model described by Eq. S, it is useful to decompose the survival and recruitment parameters as follows: $\acute{\zeta}_{it} = 1 - \delta_{it} - \eta_{it}$ and $\acute{\beta}_{it} = \lambda_{it} + \delta_{it} - 1$. The parameter δ_{it} can be thought of as a demographic turnover rate; the parameters η_{it} and λ_{it}, respectively, represent changes (positive or

negative) to survival and recruitment attributable to environmental events. This leads to

$$N_{i,t+1} \quad I_{it} + Bi\left(N_{it}, 1 - \delta_{it} - \eta_{it}\right) + Pois\left(N_{it}\left(\lambda_{it} + \delta_{it} - 1\right)\right)$$

<div align="right">(S)</div>

The reason for parameterizing the model in this way is that the component of $var\left(N_{i,t+1} - N_{i,t}\right)$ that scales with $N_{i,t}^2$ is then $var\left(\eta_{it}\right) + var\left(\lambda_{it}\right)$ (which we interpret as environmental variance, because it implies that $var\left(\left(N_{i,t+1} - N_{i,t}\right)/N_{i,t}\right)$ is constant with abundance $N_{i,t}$). The component of the variance scaling with $N_{i,t}$ (which we attribute to demographic variance) is a more complicated expression (not shown here, but see further down for the special case $\eta_{it} = 0$).

Two problems with fitting the model described by Eq. S to our data are that (i) we have no estimates of immigration rates or regional abundances for most species; and (ii) from single census intervals (i.e., time series with only two independent time points), the η_{it} and λ_{it} environmental variance parameters cannot be estimated separately (essentially because one does not know how to apportion imbalances in the survival and recruitment rates of a given species to environmental variance in the survival versus the recruitment process). Our solution to the first problem is to ignore immigration (i.e., assume $I_{it} = 0$). This will have the effect of inflating estimates of λ_{it} for rare species (because immigration will be interpreted as local population growth, and immigration is more important for rare species), and slightly inflating the overall estimate of environmental variance $var\left(\lambda_{it}\right)$.

For the second problem, there are two reasonable solutions: omit the η_{it} term, and thereby consider environmental variance only in recruitment, or omit the λ_{it} term, and thereby consider environmental variance only in survival. We followed the approach of Melbourne & Hastings ([2008](#)) and considered environmental variance only in recruitment. To justify the focus on environmental variance in recruitment, we looked at the site for which the most census intervals were available ($n = 6$ at BCI) and we calculated the mean survival rate $\acute{s}_i$ for each species i across all six intervals. The theoretical variance in survival rate for each species, if there is no environmental variance, is approximately $\sigma_{s_i}^2 = \acute{s}_i(1 - \acute{s}_i)/\acute{N}_i$ (following the binomial distribution with the mean abundance of the species $\acute{N}_i$). Taking only species with abundance ≥ 10 (for which the coefficient of variation in N_i is not too high) we found that the actual variance of the survival rate of species i across the six census intervals was $2.18\sigma_{s_i}^2$ (median), indicating the presence of environmental variance or demographic heterogeneity in the survival process. Performing a similar analysis on the recruitment rates, we found that the actual variance of the recruitment rate $\acute{l}_i$ of species i across the six census intervals was $6.81\sigma_{l_i}^2$ (median), where $\sigma_{l_i}^2 = \acute{l}_i/\acute{N}_i$. Thus, although there is environmental variance and/or demographic heterogeneity in both the survival and recruitment processes, they are much more prevalent in the recruitment process (in the BCI data).

Setting $\eta_{it}=0$ and $I_{it}=0$ then, we have the following population dynamics equation:

$$N_{i,t+1} \; Bi\left(N_{it}, 1-\delta_{it}\right)+Pois\left(N_{it}\left(\lambda_{it}+\delta_{it}-1\right)\right)$$

(S)

where δ_{it} can again be interpreted as a demographic mortality or turnover rate , and λ_{it} can be interpreted either as changes to recruitment due to environmental events or just as a population growth rate, because we have $E\left(N_{i,t+1}|N_{it}=N\right)=\lambda_{it}N$. Using the law of total variance we have

$$var\left(N_{i,t+1}|N_{it}=N\right)=N^2 var\left(\lambda_{it}\right)+N\left(E\left(\lambda_{it}\right)+2E\left(\delta_{it}\right)-E\left(\delta_{it}^2\right)-1\right)$$

(S)

and so the inter-census environmental variance ([Engen *et al.* 2005](#)) can be estimated as $var\left(\lambda_{it}\right)$ and the demographic variance as $E\left(\lambda_{it}\right)+2E\left(\delta_{it}\right)-E\left(\delta_{it}^2\right)-1$.

For mathematical convenience, we express the inter-census mortality rates δ_{it} and population growth rates λ_{it} in terms of instantaneous mortality rates μ_{it} and instantaneous population growth rates ρ_{it} so that $\delta_{it}=1-e^{-\mu_{it}\Delta T_{it}}$ and $\lambda_{it}=e^{\rho_{it}\Delta T_{it}}$. The parameters ρ_{it} and μ_{it} (the 'true' and unknowable rate constants, for which we use Greek letters) must be distinguished from the observed rate constants r_{it} and m_{it} (Eqs. S and S), for which we use Roman letters. For small ΔT_{it} , we can then use Eq. S to write

$$var\left(N_{i,t+1}|N_{it}=N\right)\approx N^2\Delta T_{it}^2 var\left(\rho\right)+N\Delta T_{it}\left(E\left(\rho\right)+2E\left(\mu\right)\right)=N^2\Delta T_{it}^2 v_e+N\Delta T_{it}v_d$$

(S)

where $v_e\equiv var\left(\rho\right)$ and $v_d\equiv E\left(\rho\right)+2E\left(\mu\right)$ are the estimates of annualized environmental and demographic variance in the main text (Table 2). Eq. 5 in the main text comes directly from Eq. S.

Given forest census data containing counts of individuals (N_{it}) and survivors (Z_{it}), and time intervals (ΔT_{it}), the model described by Eq. S can be used to estimate the distributions of μ_{it} and ρ_{it} across species (and hence the variance terms in Eq. S). We fitted models to each census interval at each site as described in Appendix S5 below. The fitting procedure was then repeated for the entire census period at each site (i.e., treating the period between the first and last census as a single long census interval) to explore the variance in abundance fluctuations on longer timescales.

Appendix S4: Derivation of asymmetric Laplace distribution of environmental variance

To derive a functional form for the distribution of intrinsic population growth rates, ρ , note that variance of population growth rates is mathematically equivalent to environmental variance in our model (Appendix S3), so that the distribution from which population growth rates are drawn should reflect environmental factors. Working first with the inter-census rates $\lambda_i \geq 0$ rather than the instantaneous rates, let the distribution of λ_i be the product of three things: a constant effect of the environment on all species in a given census measured by a parameter $\gamma \geq 0$, environmental events that increase the population growth rate following a distribution X with support i , and environmental events that decrease the population growth rate following a distribution Y with support $[0,1]$. We chose power-law distributions for X and Y ([Keitt & Stanley 1998](#); [Marquet et al. 2005](#)). Thus $P_X(x) = (\alpha-1)x^{-\alpha}$ with $\alpha > 1$ and $P_Y(y) = (\beta+1)y^{\beta}$ with $\beta > 1$. Let the distribution from which λ_i is drawn be $\Lambda = \gamma X Y$, so

$$P_\Lambda(\lambda) = \frac{1}{\gamma} \int_0^{min(1, r/\gamma)} \frac{1}{y} P_{X,Y}\left(\frac{r}{\gamma y}, y\right) dy = \frac{(\alpha-1)(\beta+1)}{(\alpha+\beta)\gamma} \times \begin{cases} \left(\dfrac{r}{\gamma}\right)^\beta, & r < \gamma \\ \left(\dfrac{r}{\gamma}\right)^{-\alpha}, & r \geq \gamma \end{cases}$$

Now to convert to the instantaneous rates set $P = \dfrac{1}{\Delta T}\log\Lambda$ and $c = \dfrac{1}{\Delta T}\log\gamma$. So

$$P_P(\rho) = a\, e^{\rho\,\Delta T} \times \begin{cases} \left(\dfrac{e^{\rho\Delta T}}{e^{c\,\Delta T}}\right)^\beta, & \rho < c \\ \left(\dfrac{e^{\rho\,\Delta T}}{e^{c\Delta T}}\right)^{-\alpha}, & \rho \geq c \end{cases} = a\, e^{c\Delta T} \times \begin{cases} e^{(\rho-c)(1+\beta)\Delta T}, & \rho < c \\ e^{(\rho-c)(1-\alpha)\Delta T}, & \rho \geq c \end{cases}$$

Redefining $-(1-\alpha)\Delta T = \phi_1$ and $(1+\beta)\Delta T = \phi_2$ and the normalization constant $k = a\, e^{c\Delta T}$, we have

$$P_P(\rho) = k \times \begin{cases} e^{(\rho-c)\phi_2}, & \rho < c \\ e^{(c-\rho)\phi_1}, & \rho \geq c \end{cases}$$

(S)

Eq. S is an asymmetric Laplace distribution and defines the distribution used for ρ in the main model.

Appendix S5: Likelihood of observations

To fit the models, we calculated likelihoods of population changes and survival given a set of model parameters. We used a hierarchical modeling approach in which there are parameters for the community-wide models describing the 'hyperdistributions' of ρ and μ , plus rate parameters ρ_i and μ_i fitted for every species. We assumed a lognormal distribution of mortality (turnover) rates ([Condit et al. 2006](#)) and an asymmetric Laplace (exponential) distribution of

population growth rates (Appendix S4). The 'true' and unknowable rate constants ρ_i and μ_i must be distinguished from the observed rate constants r_i and $m_i = -(1/\Delta T_i)\log(Z_i/N_i)$ calculated from the data (Eqs. S and S). The full hierarchical model for a single community, assuming a lognormal distribution of turnover rates μ and the asymmetric Laplace distribution (Eq. S) of ρ includes the following parameters:

- Ω and σ, the two parameters of the lognormal distribution of turnover rates;

- c, ϕ_1 and ϕ_2, the three parameters of the asymmetric Laplace distribution of population change rates;

- μ_i, a fitted turnover rate constant (equal to the mortality rate), one per species;

- ρ_i, a fitted population change rate, one per species.

The use of a hierarchical Bayesian approach allows the model to be divided into separate components, making it easier to understand and to write the likelihood functions. There are two levels in this model: The species level parameters, with distributions described by hyperparameters for the community, and the hyperparameters themselves.

All these parameters must be estimated given a data table containing N_{i+1}, N_i, Z_i and ΔT_i for every species. A typical tropical forest model thus requires fitting $2k+5 \approx 400$ to 2400 parameters. Using hierarchical Bayesian methods, it is straightforward to estimate these parameters and their confidence (credible) intervals. Confidence intervals on the population growth (ρ_i) and turnover (μ_i) parameters for rare species will necessarily be much broader than those for common species.

Likelihood functions are written separately for each species. First consider the likelihood of a particular value of the turnover rate constant μ given that Z individuals out of N_1 survived over ΔT years. We express the likelihood as a binomial probability following Condit *et al.* ([2006](#)) (we drop the species subscript i for ease of notation):

$$L(\mu|N_1, Z, \Delta T) = \binom{N_1}{Z}(e^{-\mu\Delta T})^Z (1 - e^{-\mu\Delta T})^{N_1 - Z}$$

Next consider the likelihood of a rate of population change ρ given a turnover rate μ and a population change from N_1 to N_2 over ΔT years. To facilitate fast calculation, we employ a normal approximation to this likelihood using the true mean $M = e^{\rho\Delta T} N_1$ and variance $V = (e^{\rho\Delta T} - (e^{-\mu\Delta T})^2) N_1$ of the underlying model:

$$L(\rho|N_1, N_2, \Delta T, \mu) \approx \frac{1}{\sqrt{2\pi V}} \exp\left(\frac{-(N_2 - M)^2}{2V}\right)$$

This says that the probability of observing a future population state N_2 follows a normal distribution centered on the expected future population size $M = e^{\rho \Delta T} N_1$ and with variance V that depends on population size, population growth rate ρ and turnover rate μ and the time period ΔT. The statement that the future population size N_2 is centered on $e^{\rho \Delta T} N_1$ is an empty one: it is simply the statement that the population has grown by $e^{\rho \Delta T}$. The important part of the equation is the assertion that the future population size is distributed normally with variance given approximately by V. This is the expected variance due to demographic variation, and it is necessary to know this to build the likelihood formulation and fit the parameters. We confirmed the validity of the normal approximation by simulations (not shown).

The top level of the model includes the hyperdistributions, or community-wide distributions, of all the species-level parameters μ_i and ρ_i. For ρ_i,

$$L(\Gamma, \phi_1, \phi_2 | \rho_i) = P_P(\rho_i \vee \Gamma, \phi_1, \phi_2)$$

where P_P is defined by Eq. S. For μ_i,

$$L(\Omega, \sigma | \mu_i) = P_M(\mu_i | \Omega, \sigma)$$

where P_M is the probability density function of the lognormal distribution.

The overall log-likelihood of the model in a forest of k species over a period between census j and census $j+1$ is then given by

$$LL_j = \sum_{i=1}^{k} \left[\log L(\mu_{ij} | N_{ij}, Z_{ij}) + \log L(\rho_{ij} | N_{i,j+1}, N_{ij}, \mu_{ij}) + \log L(\Gamma, \phi_1, \phi_2 | \rho_{ij}) + \log L(\Omega, \sigma | \mu_{ij}) \right]$$

To find the maximum likelihood, we used a Gibbs sampler with a Metropolis update rule, allowing each of the several hundred parameters for a single model to be updated one at a time (Gelman *et al.* 1995; Condit *et al.* 2006; Rüger *et al.* 2009). We ran the samplers for 10,000 steps and discarded the first 2000 as a burn-in (the samplers appeared to converge after 1000 steps). The mean from the last 8000 steps of the sampler was used as the best estimate for every parameter, and the 0.025 and 0.975 quantiles as the limits of 95% credible intervals.

Appendix S6: Estimating abundance fluctuations from the fitted model

If the time interval between censuses ΔT is not too large, we can approximate the variance of abundance fluctuations $var(N_2 - N_1 \vee N_1) = E((N_2 - N_1)^2 | N_1)$ by plugging the estimated values of demographic variance v_d and environmental variance v_e (Table 2 in the main text) into Eq. S. To calculate this variance more precisely for larger ΔT, or to calculate other statistics such as $E(\log((N_2 - N_1)^2) | N_1)$ (this statistic was used for Figs. 1–2 and Figs. S1–S3, because of the logarithmic axis scales), it is necessary to employ numerical methods. Given a time interval ΔT, an initial abundance N_1, and a fitted model (Appendices S2–S5), the general procedure is as follows:

(1) Generate random realizations of ρ and μ from the fitted distributions.

(2) Calculate $\lambda = e^{\rho \Delta T}$, $\delta = 1 - e^{-\mu \Delta T}$.

(3) Calculate realizations of N_2 from Eq. S.

(4) Calculate corresponding abundance changes $N_2 - N_1$.

(5) Calculate statistics on the abundance changes, e.g., $var\left(N_2 - N_1 \vee N_1\right)$ or
$E\left(\log\left[(N_2 - N_1)^2\right]\middle| N_1\right)$.

Using more realizations in step (1) leads to more precise estimates of the statistics.

References

Condit R., Ashton P., Bunyavejchewin S., Dattaraja H.S., Davies S., Esufali S., Ewango C., Foster R., Gunatilleke I., Gunatilleke C.V.S., Hall P., Harms K.E., Hart T., Hernandez C., Hubbell S., Itoh A., Kiratiprayoon S., LaFrankie J., de Lao S.L., Makana J.R., Noor M.N.S., Kassim A.R., Russo S., Sukumar R., Samper C., Suresh H.S., Tan S., Thomas S., Valencia R., Vallejo M., Villa G. & Zillio T. (2006). The importance of demographic niches to tree diversity. *Science*, 313, 98-101.

Engen S., Lande R., Saether B.E. & Weimerskirch H. (2005). Extinction in relation to demographic and environmental stochasticity in age-structured models. *Math. Biosci.*, 195, 210-227.

Gelman A., Carlin J.B., Stern H.S. & Rubin D.B. (1995). *Bayesian Data Analysis*. Chapman and Hall/CRC, Boca Raton, Florida.

Keitt T.H. & Stanley H.E. (1998). Dynamics of North American breeding bird populations. *Nature*, 393, 257-260.

Marquet P.A., Quinones R.A., Abades S., Labra F., Tognelli M., Arim M. & Rivadeneira M. (2005). Scaling and power-laws in ecological systems. *Journal of Experimental Biology*, 208, 1749-1769.

Melbourne B.A. & Hastings A. (2008). Extinction risk depends strongly on factors contributing to stochasticity. *Nature*, 454, 100-103.

Rüger N., Huth A., Hubbell S.P. & Condit R. (2009). Response of recruitment to light availability across a tropical lowland rain forest community. *Journal of Ecology*, 97, 1360-1368.

Table S1. Values of the Akaike Information Criterion (AIC) for the full fitted model, which includes asynchronous environmental variation and demographic heterogeneity, and for models that exclude one or both of these processes ("dem. het." = demographic heterogeneity; "asynch. env. het." = asynchronous environmental variance). For each site and census interval, the lowest AIC is in bold face. Note that the final two columns are models of synchronous environmental variance, in which the expected population growth rate is the same for all species in a given census interval.

		AIC			
Site and census interval		**Full model (async. env. var. + dem. het.)**	**No dem. het**	**No asynch. env. var.**	**No asynch. env. var. No dem. het.**
Edoro	1–2	**2853.9**	6144.5	9231.2	9664.3
Edoro	2–3	**2981.3**	3516.3	6267.0	7110.3
Lenda	1–2	**2538.7**	2892.4	4290.0	3975.3
Lenda	2–3	**2780.8**	3055.5	4799.1	4545.1
Pasoh	1–2	6357.8	**5655.9**	8019.5	6306.8
Pasoh	2–3	8044.3	**7044.6**	13484.2	12859.0
Pasoh	3–4	**7483.3**	9270.2	12001.9	11031.6
Pasoh	4–5	8245.0	**8040.5**	13945.5	15266.8
Lambir	1–2	11057.0	**9781.7**	16138.1	15508.9
Lambir	2–3	22897.2	**21742.4**	66209.1	73071.0
Lambir	3–4	22544.2	**20607.4**	72792.9	80643.6
Korup	1–2	**5046.4**	6175.8	17455.0	18066.2
Sinharaja	1–2	**2947.8**	7452.2	16627.8	13644.6
Sinharaja	2–3	**2168.1**	4441.4	8241.7	6529.5
Khao Chong	1–2	4704.2	**4339.6**	6512.9	7315.6
Khao Chong	2–3	4594.7	**3829.6**	5783.7	5206.4
BCI	1–2	**3176.9**	4715.3	7789.2	9403.0
BCI	2–3	**3371.6**	7429.0	11539.8	16217.9
BCI	3–4	**3090.9**	8180.6	14898.2	12470.2
BCI	4–5	**3240.2**	4173.7	11434.2	10287.3
BCI	5–6	3236.9	**2947.1**	9135.0	11675.7
BCI	6–7	3198.0	**2838.0**	10076.8	11324.8
Mudumalai	1–2	**629.6**	7182.4	3642.2	11054.8
Mudumalai	2–3	**617.1**	3933.9	2483.8	5276.7
Mudumalai	3–4	**634.7**	826.1	8566.6	11655.2
HKK	1–2	**2680.3**	5373.8	8326.5	10102.3
HKK	2–3	**4042.6**	6108.5	63422.5	61507.8
HKK	3–4	3732.4	**3306.6**	36695.7	38640.1
Palanan	1–2	3195.0	**2593.5**	18875.2	18417.8
Palanan	2–3	**2904.8**	2913.8	4373.6	4342.8
Fushan	1–2	**1172.8**	1412.2	4959.3	5541.3

Table S2. Fits of the full population model to tree population change data at each site for each census interval (supplementary to Table 2 in the main text).

| Site and census interval		Parameters for fitted population growth rate (ρ) distribution			Parameters for fitted mortality rate (μ) distribution	
		c	Φ_1	Φ_2	Ω	σ
Edoro	1–2	-0.0075	53.7	91.2	-3.930	0.829
Edoro	2–3	-0.0081	40.7	84.5	-3.710	0.796
Edoro	1–3	-0.0058	54.8	78.0	-3.871	0.857
Lenda	1–2	-0.0005	153.7	96.4	-4.024	0.818
Lenda	2–3	-0.0059	79.1	64.8	-3.661	0.711
Lenda	1–3	-0.0018	121.4	59.8	-3.812	0.779
Pasoh	1–2	-0.0107	184.8	176.0	-4.037	0.427
Pasoh	2–3	-0.0073	61.6	148.4	-3.743	0.497
Pasoh	3–4	-0.0082	196.7	80.0	-3.541	0.547
Pasoh	4–5	-0.0147	47.2	84.9	-3.497	0.506
Pasoh	1–5	-0.0088	105.4	108.1	-3.837	0.556
Lambir	1–2	0.0054	93.4	147.2	-4.350	0.700
Lambir	2–3	-0.0001	53.8	112.6	-3.853	0.654
Lambir	3–4	-0.0030	51.4	260.2	-3.881	0.474
Lambir	1–4	0.0024	77.8	150.6	-4.193	0.530
Korup	1–2	-0.0043	78.7	99.0	-4.018	0.834
Sinharaja	1–2	-0.0060	94.1	65.1	-4.019	0.766
Sinharaja	2–3	-0.0094	172.7	89.9	-3.840	0.530
Sinharaja	1–3	-0.0083	129.7	72.3	-3.902	0.636
Khaochong	1–2	-0.0036	61.3	83.1	-3.745	0.744
Khaochong	2–3	-0.0087	70.3	105.9	-3.617	0.649
Khaochong	1–3	-0.0037	83.2	71.9	-3.634	0.679
BCI	1–2	0.0072	44.2	27.4	-3.102	0.788
BCI	2–3	0.0010	40.2	40.2	-3.294	0.876
BCI	3–4	-0.0060	73.2	38.3	-3.224	0.850
BCI	4–5	-0.0185	34.3	49.6	-3.146	0.774
BCI	5–6	-0.0143	30.9	80.5	-3.235	0.776
BCI	6–7	-0.0086	28.4	95.5	-3.280	0.746
BCI	1–7	-0.0042	56.8	47.1	-3.322	0.825
Mudumalai	1–2	-0.0049	98.1	17.3	-3.004	1.061
Mudumalai	2–3	-0.0046	40.0	14.6	-3.061	1.158
Mudumalai	3–4	-0.0081	13.2	29.9	-3.660	1.286
Mudumalai	1–4	-0.0090	28.5	21.3	-3.340	1.078
HKK	1–2	-0.0074	33.2	27.7	-3.126	0.922
HKK	2–3	-0.0095	14.4	53.4	-3.633	0.784
HKK	3–4	-0.0004	16.4	55.6	-3.075	0.863
HKK	1–4	-0.0016	25.3	42.9	-3.481	0.909
Palanan	1–2	0.0125	22.1	118.8	-4.015	0.496
Palanan	2–3	-0.0123	61.3	96.5	-3.707	0.568
Palanan	1–3	0.0020	42.5	139.3	-3.892	0.498
Fushan	1–2	-0.0019	51.0	44.6	-3.664	1.001
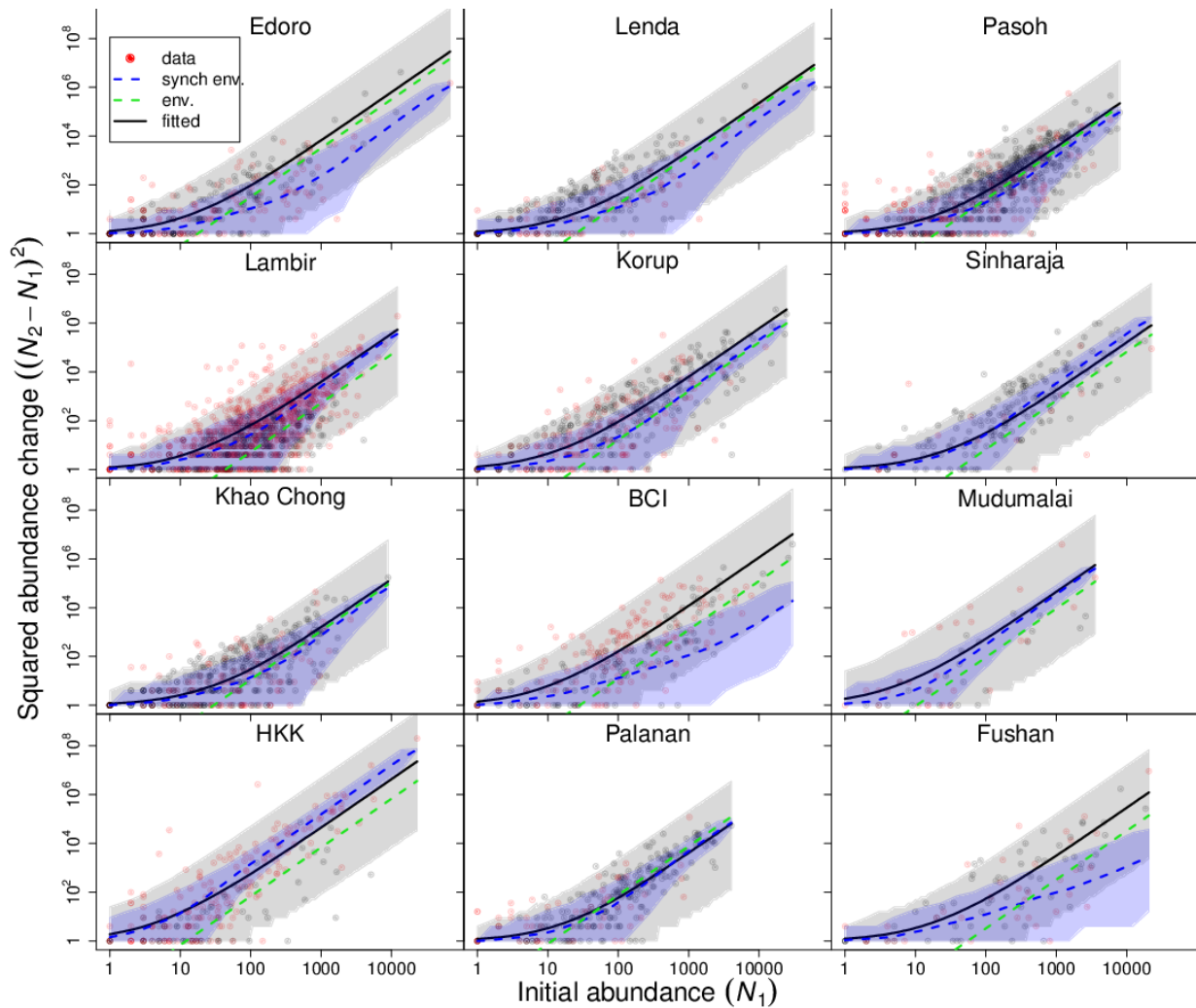
Figure S1 Squared abundance changes (vertical axes; log scale) as a function of initial abundance (horizontal axes; log scale) as in Fig. 1 in the main text but with synchronous environmental variance added to the model of demographic variance (blue dashed line with shaded 95% confidence intervals). Gray points represent decreases in abundance and red points represent increases in abundance.
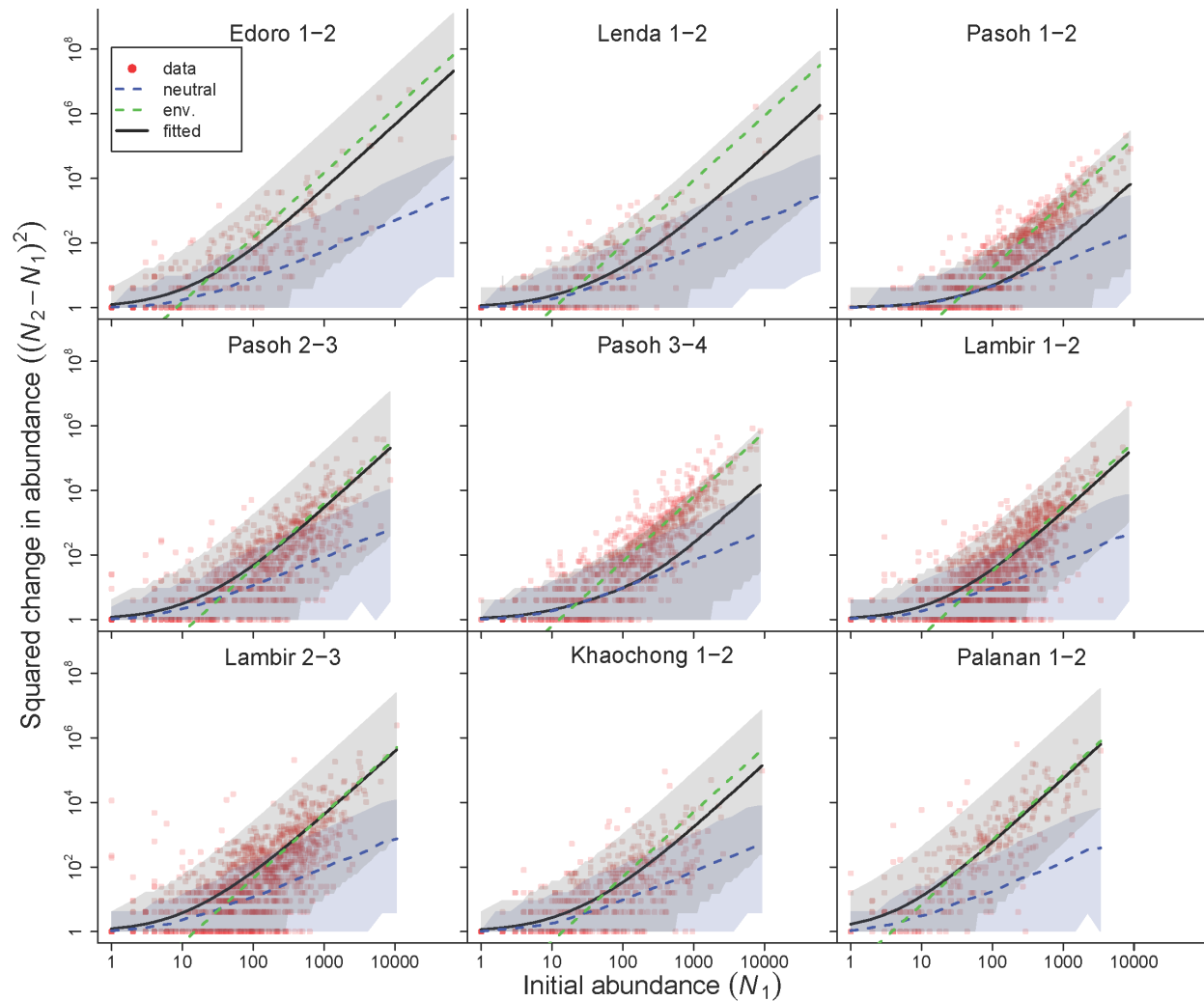
Figure S2 Squared abundance changes (vertical axes; log scale) as a function of initial abundance (horizontal axes; log scale) in the Edoro, Lenda, Pasoh, Lambir, Khao Chong and Palanan forests over different census intervals (panels; number range the census interval; see main text Fig. 1 for most recent census interval at each site). Each red point shows data for one species. Blue dashed lines with shaded 95% confidence intervals show the predictions of neutral models. Green dashed lines show a best fit power law with exponent 2.0, which corresponds to a model where the effects of environmental variance are perfectly correlated across individuals within species. Black curves with shaded 95% confidence intervals show the fitted model.
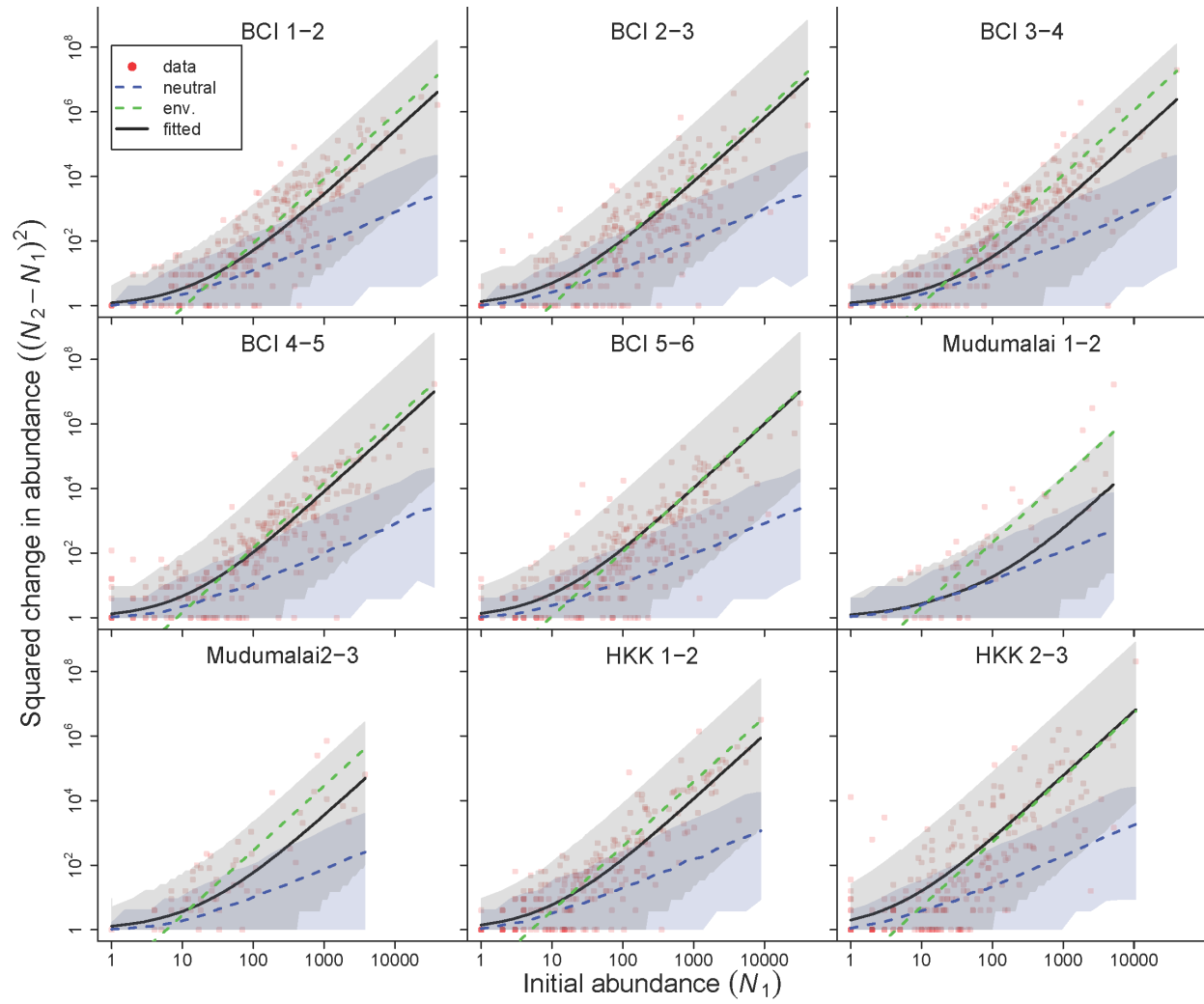
Figure S3 As for Fig. S2 but for the BCI, Mudumalai and HKK forests.